Quantum-well reflectivity and exciton-polariton dispersion

F. Tassone and F. Bassani
Scuola Normale Superiore, I-56100 Pisa, Italy

L. C. Andreani
Institut Romand de Recherche Numérique en Physique des Matériaux, PHB-Ecublens, CH-1015 Lausanne, Switzerland

(Received 12 August 1991; revised manuscript received 31 October 1991)

We prove that reflectivity measurements as a function of angle of incidence allow the measurement of the exciton-polariton modes in quantum wells. The resonant polaritons at $k_{\parallel} < k_0 = \omega/v$ manifest themselves as peaks in the reflectivity while surface polaritons at $k_{\parallel} > k_0$ manifest themselves as dips in the attenuated total reflection. A comparison of the reflectivities with polarization perpendicular and parallel to the plane of incidence allows us to detect the different polariton modes and to measure the dispersion relation. We also give expressions to compute reflectivity and transmission for the case of multiple quantum wells, including the effects of multiple reflections. Examples are given for standard reflectivity of $GaAs/Al_xGa_{1-x}As$ quantum wells and for attenuated total reflection of $CuCl/CaF_2$ quantum wells.

I. INTRODUCTION

Reflectivity measurements have proven to be a powerful tool for the study of the optical properties of semiconductors, because they allow the estimate of many important bulk parameters related to the oscillator strengths of exciton resonances.[1,2] Moreover, the use of different incidence angles and of light polarization has given information in cases when symmetry is lower than cubic, and the use of evanescent waves in attenuated total reflection experiments has allowed the excitation of surface polaritons.[3]

Recently, the study of optical properties of semiconductors was extended to quantum wells. In these structures, quantum confinement effects on electrons and holes become essential, so that a two-dimensional character is developed in their behavior. This affects the polariton states and therefore must be relevant to the reflectivity.[4,5]

In 1966 Agranovich and Dubovskii[6] proved that, when the translational symmetry is broken in one direction, the polaritons can be of two types, those with $k_{\parallel} < \omega/v$ which have a finite lifetime (resonant polaritons), and those with $k_{\parallel} > \omega/v$ which have an infinite radiative lifetime (surface polaritons). In a recent paper we have given the dispersion of polaritons in quantum wells and the lifetimes of the resonant ones,[7] thus completing previous studies by Nakayama,[8] Cho,[9] and Andreani and Bassani.[10]

The purpose of this paper is to show how these modes come separately into play in standard and attenuated total reflection and to compute the resonances to be expected in the reflectivity curves. We will show how the position and shape of the reflectivity resonances are related to the dispersion laws and the radiative linewidths of the polaritons. In the case of the usual reflectivity experiments, only resonant polaritons will be detected while surface polaritons can be excited with attenuated total reflection experiments. We calculate the reflectivity curves for polarization of the electric field both parallel and perpendicular to the plane of incidence. In the first case at oblique incidence two resonances arise from different optically active electromagnetic modes. We also calculate how the reflectivity curves are modified by the existence of a medium external to the sample and stress the limitations imposed by experimental parameters such as the barrier width, the homogeneous broadening or the angle of incidence, for both standard and attenuated total reflection.

In Sec. II we briefly review the results of Ref. 7, and also show how it is possible to describe any experimental configuration in terms of all the independent electromagnetic modes. In Sec. III we calculate the standard reflectivity of the quantum well at any angle of incidence. In Sec. IV we perform a similar calculation for the case of evanescent waves in the barriers, relevant to an attenuated total reflection (ATR) experiment. We demonstrate that attenuation resonance dips appear in the reflectivity at energies related to those of the surface polaritons. Numerical results are given for cases of interest. Discussion of the results is presented in Sec. V.

II. ELECTROMAGNETIC MODES IN A QUANTUM WELL

Following the general approach of linear response theory[11] or density matrix theory,[12] we may write the susceptibility of a quantum well arising from the existence of exciton confined states as a nonlocal function:

$$\chi_{QW}(z,z',\mathbf{k}_{\parallel},\omega)=\frac{1}{h}\sum_{\substack{n \\ \varepsilon\to 0^+}}\frac{\mu_{cv}\otimes\mu_{cv}}{\omega_n(\mathbf{k}_{\parallel})-\omega-i\varepsilon}\times|F_n(0)|^2\rho(z)\rho(z')\,, \quad (1)$$

where $\rho(z)=c_e(z)v_h(z)$ is the product of the confinement functions for electrons and holes in the well and defines

the pair of subbands of the exciton considered, μ_{cv} is the dipole matrix element in the bulk material, $F_n(0)$ is the value of the quantum-well exciton envelope function at the origin in the relative coordinate system, and $\hbar\omega_n(\mathbf{k}_\parallel)$ is the energy of the nth exciton level in the quantum well, including the short-range exchange contribution[10] and spatial dispersion. The exciton energies and the other parameters appearing in Eq. (1) can be computed from the microscopic theory; results within the effective-mass approximation have been obtained, for instance, by Andreani and Pasquarello.[13] The confinement properties of the electrons and holes are contained in $\rho(z)$, while the interaction of the exciton with light is determined by the oscillator strength per unit area of the optical transitions:

$$\bar{f}_n=\frac{f_n}{S}=\frac{2m_0\omega_0\mu_{cv}^2}{\hbar e^2}|F(0)|^2\left|\int dz\,\rho(z)\right|^2 . \tag{2}$$

Selection rules which depend on the polarization are also contained in expressions (1) and (2), and can be obtained from symmetry considerations.[14]

The present approach, which is similar to that of Ref. 8 and 9, treats the exciton-photon interaction by a nonlocal susceptibility with microscopic parameters. This is to be compared with a phenomenological model in which the quantum well is represented by a local dielectric layer.[5,15] The microscopic model is more fundamental, and does not need any additional boundary conditions in the limit of thick wells.[9] The local dielectric model usually gives similar results, but it can fail when the damping becomes too small, as discussed in Ref. 16.

If we explicitly solve Maxwell's equation

$$\nabla\times\nabla\times\mathbf{E}-\frac{\omega^2}{c^2}\left[\epsilon_\infty\mathbf{E}+4\pi\int_{-\infty}^{+\infty}dz'\chi(\omega,\mathbf{k}_\parallel,z,z')\times\mathbf{E}(\omega,\mathbf{k}_\parallel,z')\right]=0 , \tag{3}$$

with the appropriate boundary conditions at the quantum-well interfaces and at infinity, the latter ones being determined by the experimental conditions of excitation, we are able to calculate the intensity of the reflected or transmitted waves.

Since the $\rho(z)$ confinement factors are even for optically allowed transitions, it is convenient to find the solutions to the problem which have definite parity under inversion of the z coordinate. If we take the in-plane wave vector $\mathbf{k}_\parallel$ in the $\hat{\mathbf{x}}$ direction, we can first classify solutions according to their electric field polarization with respect to $\hat{\mathbf{x}}$, and within these classes we can classify the solutions according to the parity in z of the nonzero electric-field components. For polarization in the plane of incidence both E_x and E_z are nonzero, while for perpendicular polarization the only nonzero component is E_y. The four independent electromagnetic modes which result are shown in Fig. 1. The two optically active modes with even $\hat{\mathbf{y}}$ and $\hat{\mathbf{x}}$ polarization are called transverse (T) and longitudinal (L), respectively. The mode with even $\hat{\mathbf{z}}$ polarization is called the Z mode (Z).

In the case of $k_\parallel<k_0=\omega/c\sqrt{\epsilon_\infty}$ we always have traveling waves in the barrier of dielectric constant ϵ_∞, the value of k_z being real such that

$$k_z^2=k_0^2-k_\parallel^2 . \tag{4}$$

We then divide the problem into two different regions: the barrier region with $|z|>L/2$ and the well region with $|z|<L/2$. In the first region $\rho(z)\simeq 0$ so that Maxwell's equation (3) describes free traveling waves. This solution must be matched to the solution in the well region using boundary conditions at the $|z|=L/2$ surfaces. We can define a scattering amplitude α as the ratio of the amplitudes of outgoing and incoming waves. The procedure is described in Ref. 7.

For the optically active modes, we find a Breit-Wigner type scattering amplitude of the form

$$\alpha=e^{ik_zL}\frac{\omega-\bar{\omega}(\mathbf{k}_\parallel,\omega)-i\Gamma(\mathbf{k}_\parallel,\omega)}{\omega-\bar{\omega}(\mathbf{k}_\parallel,\omega)+i\Gamma(\mathbf{k}_\parallel,\omega)} , \tag{5}$$

with a resonance at

$$\omega_r=\bar{\omega}(\mathbf{k}_\parallel,\omega_r) , \tag{6}$$

and a radiative linewidth $\Gamma(\mathbf{k}_\parallel,\omega_r)$. In particular, for the modes indicated in Fig. 1, we obtain the following expressions:

$$\bar{\omega}_{\mathrm{T}}(\mathbf{k}_\parallel,\omega)=\omega(\mathbf{k}_\parallel)-4\pi\frac{\mu_{cv}^2|F(0)|^2}{\epsilon_\infty\hbar}k_0^2P(k_z) , \tag{7}$$

$$\Gamma_{\mathrm{T}}(\mathbf{k}_\parallel,\omega)=\frac{2\pi\mu_{cv}^2|F(0)|^2Q^2(k_z)}{\epsilon_\infty\hbar}\frac{k_0^2}{k_z} , \tag{8}$$

$$\bar{\omega}_{\mathrm{L}}(\mathbf{k}_\parallel,\omega)=\omega(\mathbf{k}_\parallel)-4\pi\frac{\mu_{cv}^2|F(0)|^2}{\epsilon_\infty\hbar}k_z^2P(k_z) , \tag{9}$$

$$\Gamma_{\mathrm{L}}(\mathbf{k}_\parallel,\omega)=\frac{2\pi\mu_{cv}^2|F(0)|^2Q^2(k_z)}{\epsilon_\infty\hbar}k_z , \tag{10}$$

$$\bar{\omega}_Z(\mathbf{k}_\parallel,\omega)=\omega(\mathbf{k}_\parallel)+4\pi\frac{\mu_{cv}^2|F(0)|^2}{\epsilon_\infty\hbar}\left[\int dz\,\rho^2(z)-\mathbf{k}_\parallel^2P(k_z)\right], \tag{11}$$

$$\Gamma_Z(\mathbf{k}_\parallel,\omega)=\frac{2\pi\mu_{cv}^2|F(0)|^2Q^2(k_z)}{\epsilon_\infty\hbar}\frac{\mathbf{k}_\parallel^2}{k_z} , \tag{12}$$

where

$$Q(k_z)=\int_{-L/2}^{+L/2}dz\,\rho(z)\cos(k_zz) , \tag{13}$$

$$P(k_z)=-\int_{-L/2}^{+L/2}dz\int_{-L/2}^{+L/2}dz'\frac{1}{2k_z}\sin(k_z|z-z'|)\times\rho(z)\rho(z') . \tag{14}$$

The solution for the antisymmetric mode [(B) of Fig. 1] is easily found because there is no polarization contribution from the quantum well. We obtain

$$\alpha_{\mathrm{T,as}}=e^{ik_zL} . \tag{15}$$

When $k_\parallel>k_0$, condition (4) leads to k_z pure imaginary ($k_z=i\kappa_z$), so that only evanescent waves can exist in the barrier. In this case the resonances are similar to those of

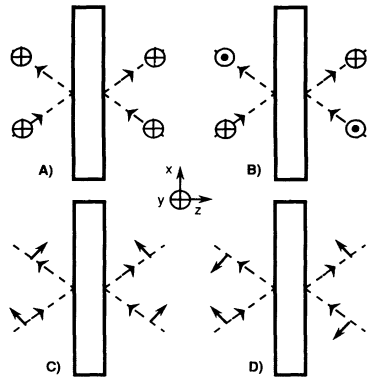

FIG. 1. Schematic illustration of the four independent electromagnetic modes: (A) y polarized (even), (B) y polarized (odd), (C) E_x even, E_z odd, (D) E_z even, E_x odd. The dashed lines represent propagation direction of the optical waves in the barrier and the solid lines with arrows the electric-field directions; the circles represent $\hat{\mathbf{y}}$ vectors going into the paper ($\hat{\mathbf{x}},\hat{\mathbf{y}}$ plane), or out of it if the circle contains a cross or a dot, respectively.

surface states and have been called quantum-well surface polaritons. These modes have zero radiative linewidth. Their dispersion laws are given again by Eqs. (6), (7), (9), and (11), provided the expression for $P(k_z)$ is replaced by

$$\bar{P}(\kappa_z)=\int_{-L/2}^{+L/2}dz\int_{-L/2}^{+L/2}dz'\frac{1}{2\kappa_z}e^{-\kappa_z|z-z'|}\rho(z)\rho(z') \ . \tag{16}$$

We wish to remark that the above results take into account the interaction of the electronic excitations with the electromagnetic field, including retardation. As shown in Ref. 10, the long-range electron-hole exchange of the microscopic theory represents the interaction with the electromagnetic field in the instantaneous approximation ($c\rightarrow\infty$) and is responsible for the internal structure (separation of the exciton modes). The effect of considering retardation is to introduce a discontinuity in the dispersion relation at $k_{\parallel}=k_0$, and to give rise to resonances with finite radiative lifetime for $k_{\parallel}<k_0$. It appears that the differences occur in the vicinity of $k_{\parallel}=k_0$; for large values of $k_{\parallel}$ the retarded radiative correction coincides with that obtained from the long-range e-h exchange. The situation is exemplified in Fig. 2 for the case of $GaAs/Ga_{1-x}Al_xAs$ quantum wells; we can observe the crossing between the L and Z modes at a high value of $k_{\parallel}$, and the approaching of the Z mode to the T mode as $k_{\parallel}$ increases.

It may also be of interest to compare the quantum-well polariton modes with the surface polariton modes which appear at the interface of a semi-infinite medium. They bear similarities because in both cases the translational symmetry is broken in one direction and the good quantum number is $k_{\parallel}$, but they also differ because in the interface case the Green's function corresponding to expression (1) contains the bulk excitons, as shown by Maradudin and Mills[17] and Cho.[9] The most important difference is the existence of resonant polaritons in the quantum well, which makes possible a coupling with traveling electromagnetic waves. Another significant

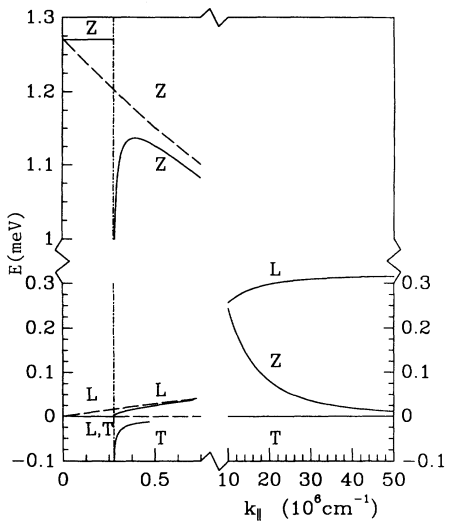

FIG. 2. Comparison of the dispersion due to the long-range e-h exchange (dashed line) and that due to the full electromagnetic interaction with retardation (solid line). The case of a 60-Å-wide $GaAs/Ga_{1-x}Al_xAs$ quantum well (with $x=0.4$) is considered. The oscillator strength $f_{xy}=f_z/4=35\times10^{-5}$ Å^{-2} from Ref. 13 has been used. Energies are referred to the exciton energy ($E_{\rm exc}\simeq1.6$ eV) without center-of-mass dispersion.

difference is the existence of the T mode in the quantum well.

A useful comparison may be with the modes in a thin slab. Kloos[18] proved that when two surfaces are separated by a thin slab of metallic material the two surface plasmon polaritons interact and produce both the L mode and Z plasmon polariton mode. This also occurs for excitons in a thin semiconductor slab, with results qualitatively similar to those described above. A quantitative analysis however requires the use of nonlocal susceptibility and the microscopic calculation of confined excitons.

The above described independent modes are sufficient to interpret a number of physical effects related to the behavior of the electromagnetic radiation interacting with the medium. In particular, an appropriate combination of symmetric and antisymmetric modes produces the situation of an incoming beam partly reflected and partly transmitted. In the next two sections we will show how the experimental reflection and transmission coefficients are related to the polariton modes and allow their measurement.

III. STANDARD REFLECTIVITY AND RESONANT POLARITONS

We show in Fig. 3 that the addition of the odd and even modes for a definite polarization leaves only one incoming wave on the quantum well, together with the reflected and transmitted beams. The reflectivity and transmission coefficients for perpendicular polarization are

$$r^s_{\rm QW}=\tfrac{1}{2}(\alpha_{{\rm T},s}-\alpha_{{\rm T},as}),\quad t^s_{\rm QW}=\tfrac{1}{2}(\alpha_{{\rm T},s}+\alpha_{{\rm T},as}) \ , \tag{17}$$

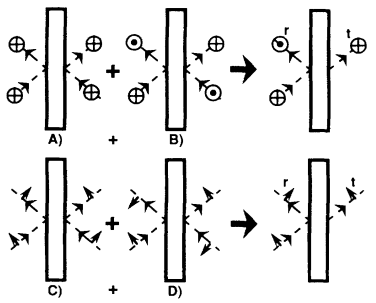

FIG. 3. Superposition of even and odd modes to obtain quantum-well reflectivity and transmission for perpendicular polarization and parallel polarization.

and for parallel polarization

$$r^p_{\rm QW}=\tfrac{1}{2}(\alpha_{\rm L}-\alpha_Z),\quad t^p_{\rm QW}=\tfrac{1}{2}(\alpha_{\rm L}+\alpha_Z)\ . \tag{18}$$

Taking into account the Breit-Wigner–type form (5) for the α_s coefficients, it is easily seen that $|r^s_{\rm QW}|^2$ has a single Lorentzian resonance, whose resonance energy is given by the condition (6), and whose width is the radiative linewidth introduced in (8). Equation (7) gives the dispersion law of the resonant polaritons, so that it is possible to determine the dispersion law of the transverse resonant polariton together with its radiative linewidth from the reflectivity measurements at various angles.

For parallel polarization we have two resonances relative to the L and Z modes, respectively, as seen from expression (18). These resonances are separated in frequency by the first factor in parenthesis of (11), proportional to $\int dz\,\rho^2(z)$, the other factor being very small in the radiative region we are considering. However, they can be simultaneously seen in the reflectivity curves only using incidence angles which are neither perpendicular nor grazing. At normal incidence we have $k_\parallel=0,\Gamma_Z=0$, and for this reason the Z mode is optically inactive. In this case the scattering amplitude α_Z is also given by (15). At grazing incidence only the Z mode is optically active. The general trend at increasing incidence angles from normal to grazing incidence is a gain of strength of the Z mode and a loss of the L mode.

In order to take into account another kind of relaxation process, like the interaction with phonons, for example, we introduce a phenomenological damping parameter γ, using $\omega+i\gamma$ in the denominator of (1) instead of ω alone. We do not give here the full expressions for $|r^p_{\rm QW}|^2$ and $|r^s_{\rm QW}|^2$ obtained from (17) and (18) because in real experiments the background reflectivity from the barrier–external-medium interface always has to be taken into account. When this is done, as in the typical experimental scheme shown in Fig. 4, considering also multiple reflection, we obtain

$$|r^s_{\rm tot}|^2=\left|\frac{r^s_{12}+r^s_{\rm QW}e^{i\phi}}{1+r^s_{12}r^s_{\rm QW}e^{i\phi}}\right|^2, \tag{19}$$

$$|r^p_{\rm tot}|^2=\left|\frac{r^p_{12}+r^p_{\rm QW}e^{i\phi}}{1+r^p_{12}r^p_{\rm QW}e^{i\phi}}\right|^2, \tag{20}$$

where

$$r^s_{12}=\frac{k_{z,\rm ext}-k_z}{k_{z,\rm ext}+k_z}\ , \tag{21}$$

$$r^p_{12}=\frac{\epsilon_{\rm ext}k_z-\epsilon_\infty k_{z,\rm ext}}{\epsilon_\infty k_{z,\rm ext}+\epsilon_{\rm ext}k_z}\ , \tag{22}$$

$$k_{z,\rm ext}=\frac{\omega}{c}\sqrt{\epsilon_{\rm ext}}\cos\theta\ ,$$

$$k_z=\frac{\omega}{c}\sqrt{\epsilon_\infty-\epsilon_{\rm ext}\sin^2\theta}$$

are the external-material–to–barrier reflectivities in perpendicular and parallel polarization, respectively, θ is the incidence angle in the external material, $\epsilon_{\rm ext}$ its dielectric constant, assumed real, and $\phi=2k_zD$ is the phase gained by the electromagnetic wave in the barrier region of width D. If $\epsilon_{\rm ext}>\epsilon_\infty$, the incidence angles have to be limited to $\theta<\theta_{\rm limit}=\sin^{-1}\sqrt{\epsilon_\infty/\epsilon_{\rm ext}}$. In the case of a single quantum well we may usually neglect multiple reflections and expand in powers of $r_{\rm QW}$, which is small when the broadening is bigger than the radiative linewidths involved. In this case, using $|r_{\rm QW}|\ll 1$ we obtain an explicit expression for $|r_{\rm tot}|^2$ for the two polarizations:

$$|r^s_{\rm tot}|^2\simeq(r^s_{12})^2-2[1-(r^s_{12})^2]\frac{(\Gamma_{\rm T}+\gamma)\cos\phi+(\omega_{\rm T}-\omega)\sin\phi}{(\omega-\omega_{\rm T})^2+(\Gamma_{\rm T}+\gamma)^2}\Gamma_{\rm T}\ , \tag{23}$$

$$|r^p_{\rm tot}|^2\simeq(r^p_{12})^2-2[1-(r^p_{12})^2]\left[\frac{(\Gamma_{\rm L}+\gamma)\cos\phi+(\omega_{\rm L}-\omega)\sin\phi}{(\omega-\omega_{\rm L})^2+(\Gamma_{\rm L}+\gamma)^2}\Gamma_{\rm L}-\frac{(\Gamma_Z+\gamma)\cos\phi+(\omega_Z-\omega)\sin\phi}{(\omega-\omega_Z)^2+(\Gamma_Z+\gamma)^2}\Gamma_Z\right]\ . \tag{24}$$

Expression (23) reduces to the one already given in Ref. 16 for perpendicular incidence, while it is possible to see from (24) that if the L and Z resonances are separated by more than the broadening γ, then the ratio of the two peak heights is given by the ratio of the respective *radiative* linewidths. It can also be seen that the peak heights in the reflectivity curves are a direct measure of the ratio of the radiative linewidths to the total broadening, a parameter which can be extracted from the same data.

From the above procedure we conclude that all parameters concerning the resonant polaritons at different $k_\parallel$ can be measured simultaneously in a standard reflectivity measurement, provided that the incidence angle, the frequency, and the polarization are suitably scanned.

The reflectivity from a multiple-quantum-well (MQW) structure can be calculated following the same guidelines,

in which case multiple reflections must be considered. We consider a structure of N wells limited on both sides by overlayer barriers of thickness D, also equal to the thickness of the barriers between the wells. In each layer between the quantum well and in the barriers we have two electromagnetic waves of amplitude $E_1^{(n)}, E_2^{(n)}$ (n labeling the layer considered) traveling in opposite directions. The reflection and transmission coefficients of the whole structure can be determined by the reflection and transmission coefficient at each boundary:

$$
\begin{aligned}
& r_{\mathrm{MQW}} = r_{12} + t_{21} E_2^{(0)} , \\
& E_1^{(0)} = t_{12} + r_{21} E_2^{(0)} ; \\
& \cdots ; \\
& E_1^{(n)} = t_{\mathrm{QW}} E_1^{(n-1)} e^{i\phi} + r_{\mathrm{QW}} E_2^{(n)} , \\
& E_2^{(n-1)} e^{-i\phi} = t_{\mathrm{QW}} E_2^{(n)} + r_{\mathrm{QW}} E_1^{(n-1)} e^{i\phi} ; \\
& \cdots ; \\
& t_{\mathrm{MQW}} = t_{21} E_1^{(N)} e^{i\phi} , \\
& E_2^{(N)} e^{-i\phi} = r_{21} E_1^{(N)} e^{i\phi} ; \quad n = 1,2,\ldots,N ,
\end{aligned}
\tag{25}
$$

where it is understood that s coefficients must be used when considering perpendicular polarization and p coefficients in the other case. This system of $2N+4$ equations in $2N+4$ variables can be easily solved for r_{MQW} and t_{MQW} and generalized to systems with a more complicated geometry, e.g., with different barrier thicknesses.

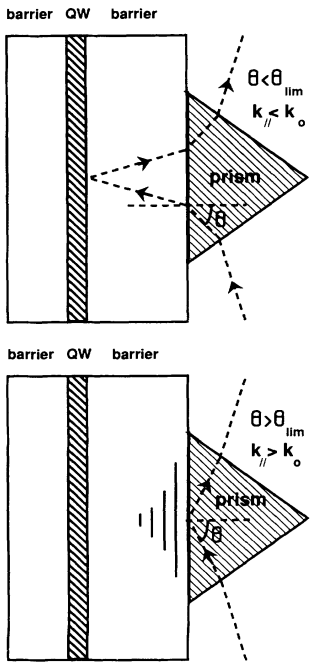

FIG. 4. A realistic schematization of a quantum-well reflectivity experiment. The barrier space, of thickness D, is limited on the right by the existence of an external prism with dielectric constant ϵ_{ext}. Both cases of standard reflection and attenuated total reflection are indicated.

We have carried out numerical calculations in order to analyze the effect of MQW's in comparison with that of the single QW. The position and the width of the reflectivity peak do not change, but the height of the peak is increased and is proportional to the number of wells (unless the total thickness of the MQW structure is comparable to the wavelength of light, in which case interference effects appear).

For the purpose of illustration we present in Fig. 5 the reflectivity of a single quantum well of $GaAs/Ga_{1-x}Al_xAs$ with an external prism of ZnSe including both the heavy-hole (HH) exciton and the light-hole (LH) exciton used as independent contributions to the susceptibility (1), with their respective oscillator strengths (2). It can be noticed that for perpendicular polarization $R_s = |r_s|^2$ shows two peaks corresponding to the transverse HH and LH excitons. For parallel polarization $R_p = |r_p|^2$ shows a small structure in correspondence with the longitudinal HH exciton and an unresolved doublet of high intensity in correspondence to the LH exciton (L and Z exciton). We recall that the HH exciton is forbidden for z polarization.[14] The separation between the Z- and T-polarized LH excitons is about 1.2 meV for a well width of 60 Å, as shown in Fig. 2.

Transmission and photoluminescence excitation experiments on multiple $GaAs/Al_xGa_{1-x}As$ quantum wells with perpendicular and parallel polarization have been carried out by Fröhlich *et al.*[19] using a ZnSe prism to achieve an incidence angle of 45° on the quantum well. The absorption spectra show peaks in correspondence to the heavy-hole and the light-hole resonant exciton polaritons as in our Fig. 5. The comparison of the parallel and perpendicular polarization absorption shows no displace-

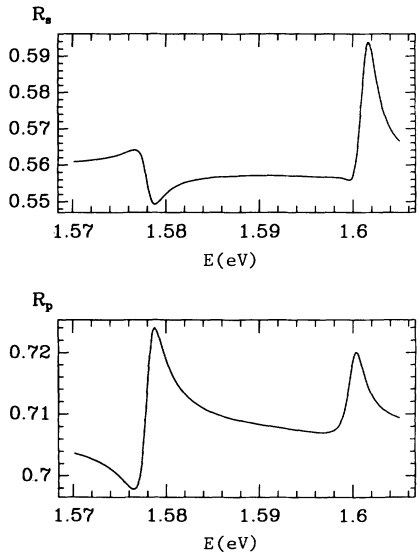

FIG. 5. Reflectivity of a single GaAs quantum-well structure with an external prism of ZnSe ($n = 2.4$), for perpendicular (R_s) and parallel (R_p) polarization at nearly grazing incidence ($\theta \simeq 90°$ in Fig. 4). Quantum-well parameters for the LH exciton are as in Fig. 2, and for the HH exciton an oscillator strength of 70×10^{-5} Å^{-2} has been used.

ment of the peak for the HH exciton polariton and a displacement to higher energy with parallel polarization by about 1.2 meV for the LH exciton polariton, in agreement with our results.

Equivalent results have been obtained by Berz *et al.*,[20] who injected the exciting light on a cleaved surface perpendicular to the quantum-well plane and therefore could excite the T and Z polaritons depending on the polarization, with $k_{\parallel} \simeq k_0$.

IV. ATTENUATED TOTAL REFLECTION AND THE DISPERSION OF THE SURFACE POLARITONS

In Sec. III we showed how standard reflectivity measurements can be made using an external prism having $\varepsilon_{\text{ext}} > \epsilon_\infty$, provided the angle of incidence is smaller than the limit angle at which total reflection occurs. If one goes beyond this angle, evanescent waves in the z direction are produced in the barrier region. Surface polaritons are characterized by evanescent waves in the barrier, and are expected to produce reflectivity at angles and frequencies which are related to their dispersion. Another possibility to excite surface polaritons is to scatter the incident beam on a grating of period d much smaller than the electromagnetic field wavelength. The scattered waves in the barrier, having $k'_{\parallel} = k_{\parallel} + \Delta k_{\parallel}$, with $\Delta k_{\parallel} = n(2\pi/d)$, will have $k'_{\parallel} > k_0$ as required for surface polaritons.

To calculate the ATR spectrum, we introduce as before scattering coefficients to take into account the appropriate boundary conditions. In this case k_z is purely imaginary and we use $k_z = i\kappa_z$. For the symmetric T mode, with the method explained in Ref. 7, we obtain

$$\begin{aligned}(E_y^{\text{inc}} + E_y^{\text{out}})|_{z=L/2^+} &= E_y|_{z=L/2^-} \\ \partial_z(E_y^{\text{inc}} + E_y^{\text{out}})|_{z=L/2^+} &= \kappa_z(E_y^{\text{inc}} - E_y^{\text{out}})|_{z=L/2^+} \\ &= \partial_z E_y|_{z=L/2^-}\end{aligned} \tag{26}$$

and

$$\alpha_{\text{T}} = \frac{E_y^{\text{out}}}{E_y^{\text{inc}}} = \left. \frac{E_y - \frac{1}{\kappa_z}\partial_z E_y}{E_y + \frac{1}{\kappa_z}\partial_z E_y} \right|_{z=L/2^-} . \tag{27}$$

The analytic form for the solution in the $|z| < L/2$ region is

$$E_y = \int dz' \frac{1}{2\kappa_z} e^{-\kappa_z|z-z'|}\rho(z') + A(\omega,\kappa_z)\cosh(\kappa_z z) , \tag{28}$$

where the A coefficient satisfies the condition

$$1 = 4\pi \frac{k_0^2}{\epsilon_\infty} \frac{1}{\hbar} \frac{\mu_{cv}^2 |F(0)|^2}{\omega(\mathbf{k}_{\parallel}) - \omega - i\varepsilon} [A(\omega,\kappa_z)\bar{Q}(\kappa_z) + \bar{P}(\kappa_z)] , \tag{29}$$

with

$$\bar{Q}(\kappa_z) = \int_{-L/2}^{+L/2} dz\, \rho(z)\cosh(\kappa_z z) , \tag{30}$$

and $\bar{P}$ already given in (16). Substituting A into (28) and (27), we obtain

$$\alpha_{\text{T}} = e^{-\kappa_z L} \frac{\bar{\omega}_T(\mathbf{k}_{\parallel},\omega) - \omega - i\epsilon - \frac{4\pi}{\hbar\epsilon_\infty}\bar{Q}^2\mu_{cv}^2|F(0)|^2\frac{k_0^2}{\kappa_z}}{\bar{\omega}_T(\mathbf{k}_{\parallel},\omega) - \omega - i\varepsilon} , \tag{31}$$

where the definition of the $\bar{\omega}$ is the same as in (7), provided that we use $\bar{P}$ in place of P.

The important feature of (31) is the pole at the surface polariton frequency, which produces a pole also in the reflectivity amplitude r_{QW}. Nevertheless, it is physically clear that the *total* reflectivity remains finite, and in particular $|r_{\text{tot}}|^2 = 1$ unless some channel for dissipation other than the radiative one is taken into account in the calculation, because the transmitted energy flux is zero. This requires the use of the full expression (19) with the inclusion of damping to calculate r_{tot}. If we recall the definition (21) of r_{12}^s, where we must now use the imaginary values k_z, we obtain $|r_{12}^s| = 1$, and we can use this property to transform (19) into the following:

$$r_{\text{tot}}^s = r_{12}^s \frac{1 + (r_{12}^s)^* r_{\text{QW}}^s e^{-\phi}}{1 + r_{12}^s r_{\text{QW}}^s e^{-\phi}} , \quad \phi = 2\kappa_2 D . \tag{32}$$

We can write the above equation more clearly:

$$r_{\text{tot}}^s \equiv r_{12}^s \frac{\bar{\omega}_{\text{T}}(\mathbf{k}_{\parallel},\omega) + \delta\omega_{\text{T}}(\mathbf{k}_{\parallel},\omega) - \omega - i\gamma + i\tilde{\Gamma}_{\text{T}}}{\bar{\omega}_{\text{T}}(\mathbf{k}_{\parallel},\omega) + \delta\omega_{\text{T}}(\mathbf{k}_{\parallel},\omega) - \omega - i\gamma - i\tilde{\Gamma}_{\text{T}}} , \tag{33}$$

where

$$\tilde{\Gamma}_{\text{T}} = -\text{Im}\left[r_{12}^s e^{-\phi} \frac{2\pi}{\hbar\epsilon_\infty} \bar{Q}^2 \mu_{cv}^2 |F(0)|^2 \frac{k_0^2}{\kappa_z} \right] , \tag{34}$$

$$\delta\omega_{\text{T}}(\mathbf{k}_{\parallel},\omega) = \text{Re}\left[r_{12}^s e^{-\phi} \frac{2\pi}{\hbar\epsilon_\infty} \bar{Q}^2 \mu_{cv}^2 |F(0)|^2 \frac{k_0^2}{\kappa_z} \right] . \tag{35}$$

We notice that $\tilde{\Gamma}$ is positive and, apart from the two factors which account for attenuation in the barrier and coupling to the external prism, its form is quite similar to that of the linewidth introduced in the radiative region. We also notice the appearance of the frequency shift $\delta\omega_T(\mathbf{k}_{\parallel},\omega)$. The effective surface polariton dispersion is obtained by solving the equation

$$\bar{\omega}_{\text{T}}(\mathbf{k}_{\parallel},\omega) + \delta\omega_{\text{T}}(\mathbf{k}_{\parallel},\omega) = \omega . \tag{36}$$

It is also evident that if $\gamma = 0$, then $|r_{\text{tot}}| = 1$, as we already anticipated. Taking the reflectivity $|r_{\text{tot}}|^2$ from (33), we find a Lorentzian resonance dip, with the effective resonance frequency (36), and a width given by the sum of the homogeneous broadening γ and the "radiative" linewidth $\tilde{\Gamma}$.

Similar calculations can be repeated for the L and Z modes to obtain the attenuated total reflection for the parallel polarization. We obtain

$$\alpha_L = e^{-\kappa_z L} \frac{\bar{\omega}_L(\mathbf{k}_\parallel,\omega)-\omega-i\varepsilon+\frac{4\pi}{\hbar\epsilon_\infty}\bar{Q}^2\mu_{cv}^2|F(0)|^2\kappa_z}{\bar{\omega}_L(\mathbf{k}_\parallel,\omega)-\omega-i\varepsilon}, \tag{37}$$

$$\alpha_Z = e^{-\kappa_x L} \frac{\bar{\omega}_Z(\mathbf{k}_\parallel,\omega)-\omega-i\epsilon-\frac{4\pi}{\hbar\epsilon_\infty}\bar{Q}^2\mu_{cv}^2|F(0)|^2\frac{k_\parallel^2}{\kappa_z}}{\bar{\omega}_z(\mathbf{k}_\parallel,\omega)-\omega-i\varepsilon}, \tag{38}$$

$$r_{\rm tot}^p = r_{12}^p \frac{1+(r_{12}^p)^* r_{\rm QW}^p e^{-\phi}}{1+r_{12}^p r_{\rm QW}^p e^{-\phi}}, \quad \phi = 2\kappa_z D , \tag{39}$$

where r_{12}^p has to be calculated using the imaginary valued k_z in (21), and $r_{\rm QW}^p$ combining α_L and α_Z as in Eq. (18). We can define the radiative shifts $\delta\omega_Z$ and $\delta\omega_L$ and radiative widths $\tilde{\Gamma}_Z$ and $\tilde{\Gamma}_L$ as we did for the T mode:

$$\delta\omega_L = -{\rm Re}(r_{12}^p)e^{-\phi}\frac{2\pi}{\hbar\epsilon_\infty}\bar{Q}^2\mu_{cv}^2|F(0)|^2\kappa_z , \tag{40}$$

$$\tilde{\Gamma}_L = {\rm Im}(r_{12}^p)e^{-\phi}\frac{2\pi}{\hbar\epsilon_\infty}\bar{Q}^2\mu_{cv}^2|F(0)|^2\kappa_z , \tag{41}$$

$$\delta\omega_Z = -{\rm Re}(r_{12}^p)e^{-\phi}\frac{2\pi}{\hbar\epsilon_\infty}\bar{Q}^2\mu_{cv}^2|F(0)|^2\frac{k_\parallel^2}{\kappa_z} , \tag{42}$$

$$\tilde{\Gamma}_Z = {\rm Im}(r_{12}^p)e^{-\phi}\frac{2\pi}{\hbar\epsilon_\infty}\bar{Q}^2\mu_{cv}^2|F(0)|^2\frac{k_\parallel^2}{\kappa_z} . \tag{43}$$

It is again evident that if $r_{\rm QW}^p$ is real, i.e., $\gamma=0$, then $|r_{\rm tot}^p|=1$, but two dips appear when $\gamma\neq 0$ and they can be resolved if γ is smaller than $\omega_L-\omega_Z$. The relative strength of the two modes relates to the ratio of $\tilde{\Gamma}_L$ to $\tilde{\Gamma}_Z$ as in the standard reflectivity case. Also in this case we could consider the MQW structure as in Eq. (25), and we expect a similar increase in the peak intensity unless the barrier between the wells is wider than $1/\kappa_z$.

To exemplify the attenuated total reflection we consider a CuCl quantum well with a CaF_2 barrier, as grown by Segawa *et al.*,[21] and a glass prism ($n=1.7$). The following parameters are used for a CuCl quantum well of 20 Å thickness: $m_e+m_h=2.5m_0$, $\hbar\omega_0=3.4$ eV according to the experimental results of Hönerlage, Bivas, and Duy Phach.[22] In this case the valence band is the Γ_7 nondegenerate state and the Z polarization is allowed. The separation between the three active exciton states (L, T, and Z) is given in Ref. 7 for all values of $k_\parallel$. They all contribute to the susceptibility. The computed oscillator strength per unit area is $\tilde{f}_{xy}=\tilde{f}_z=2.5\times10^{-3}$ Å^{-2} (Ref. 7).

We report in Fig. 6 the dependence of the effective linewidths $\tilde{\Gamma}_L$, $\tilde{\Gamma}_Z$, and $\tilde{\Gamma}_T$ on the corresponding wave vector for the condition of attenuated total reflection. The value of the linewidth depends on the experimental configuration and is brought about by the barrier–external-medium interface. In particular the linewidth vanishes for thick barriers, due to the factor $e^{-\phi}$.

We similarly report in Fig. 7 the shifts in surface polariton dispersion for the three active modes as functions of $k_\parallel$ as given by Eqs. (35), (40), and (42).

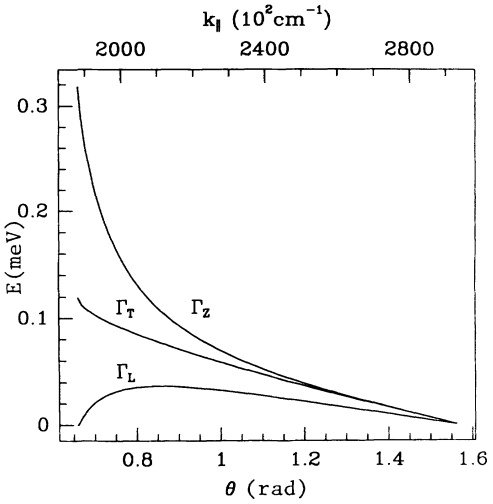

FIG. 6. "Radiative" broadenings in an attenuated-total-reflection experiment on a CuCl quantum well of 20 Å width with a 90-Å-thick barrier as function of the angle of incidence from $\theta_{\rm lim}$ to grazing incidence. The corresponding $k_\parallel$ values are also indicated. The parameters used are given in the text.

The computed curves for the attenuated total reflection on a single quantum well at nearly grazing incidence are presented in Fig. 8. It can be noticed that a dip appears in the total reflectivity in correspondence to the excitation of the surface polaritons. This is displaced with respect to the energy of the polariton dispersion curves by a quantity which depends on the experimental setup as shown in Fig. 7 for the case of interest. Also in this regime we can notice a strong difference between R_s and R_p, the latter containing two dips, one due to the L exciton, the other to the contribution of the Z mode, which has the largest strength and is appreciably shifted with

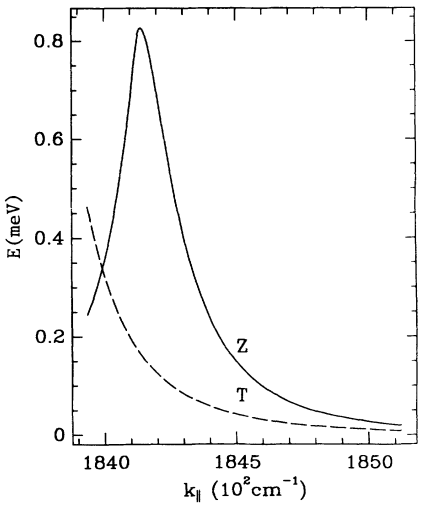

FIG. 7. Frequency shifts of the T and Z mode surface polariton in an attenuated-total-reflection experiment on a CuCl quantum well, as functions of $k_\parallel$. Parameters are as in Fig. 6, but the barrier thickness is $D=1$ μm. The frequency shift is negligible for the L mode.

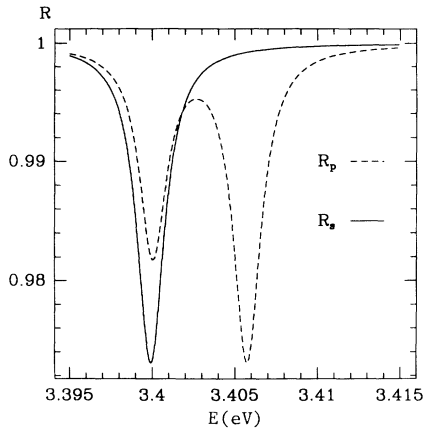

FIG. 8. Attenuated total reflectivity of a single quantum well of CuCl for parallel and perpendicular polarization at nearly grazing incidence. Parameters as in Fig. 6.

respect to the T mode.

When the angle of incidence decreases the position of the dips in R_s and R_p will be displaced in accordance with the effective dispersion curves of the polariton and this should allow a determination of the dispersion law of the surface exciton polariton modes. Of course, near the limit angle the reflectivity peak is strongly modified because of the very large increase in the radiative linewidth, and this will provide the most stringent test of the above theory.

To our knowledge, the only available experiment which detects surface exciton polaritons in $GaAs/Ga_{1-x}Al_xAs$ quantum well is due to Kohl *et al.*[15] With the use of a grating superimposed on the multiple-quantum well they observe in the zero-order diffraction the resonant HH polariton and in third-order diffraction with parallel polarization the surface polariton. With perpendicular polarization the transverse surface polariton is not resolved, probably because of the anisotropy in the coupling of the radiation with the surface grating.

V. DISCUSSION

The main results that we have obtained in the preceding sections can be summarized as follows.

The dispersion relation of resonant ($k_{\parallel} < k_0$) and surface ($k_{\parallel} > k_0$) polaritons has been obtained, together with the radiative linewidths of the resonant modes.

We have shown that it is possible to measure the dispersion of quantum-well polaritons by transmission and reflectivity experiments with polarized light. For stationary polaritons the experimental condition of attenuated total reflection is shown to be required, and the connection between the attenuation dip and the excitation energy is established.

The analysis of the line shape allows a measure of the radiative lifetime and of the total lifetime. The internal structure of the polariton can be resolved and the longitudinal and transverse polariton can be separated. With the external prism reflectivity the Z polariton can also be observed.

In the case of multiple quantum wells the effect of standard reflectivity is enhanced by multiple reflections.

ACKNOWLEDGMENTS

This work was supported by Consiglio Nazionale delle Ricerche (CNR) through a GNSM contract. One of the authors (L.C.A.) was supported in part by the Swiss National Science Foundation under Grant No. 20-5446.87. The authors are deeply indebted to Professor D. Fröhlich for communicating his data prior to publication. Useful suggestions from Professor D. Heitmann are gratefully acknowledged.

[1]L. D. Greenaway and G. Harbeke, *Optical Properties of Semiconductors* (Pergamon, Oxford, 1964).

[2]L. Schultheis and I. Balslev, Phys. Rev. B **28**, 2292 (1983); L. Schultheis and J. Lagois, *ibid.* **29**, 6784 (1984).

[3]*Surface Polaritons,* edited by V. M. Agranovich and D. L. Mills (North-Holland, Amsterdam, 1983).

[4]L. Schultheis and K. Ploog, Phys. Rev. B **30**, 1090 (1984).

[5]E. L. Ivchenko, V. P. Kochereshko, P.S. Kopev, V. A. Kosobukin, I. N. Ural'tsev, and P. R. Yakovlev, Solid State Commun. **70**, 529 (1989).

[6]V. M. Agranovich and O. A. Dubovskii, Pis'ma Zh. Eksp. Teor. Fiz. **3**, 345 (1966) [JETP Lett. **3**, 223 (1966)].

[7]F. Tassone, F. Bassani, and L. C. Andreani, Nuovo Cimento D **12**, 1673 (1990).

[8]M. Nakayama, Solid State Commun. **55**, 1053 (1985).

[9]K. Cho, J. Phys. Soc. Jpn. **55**, 4113 (1986).

[10]L. C. Andreani and F. Bassani, Phys. Rev. B **41**, 7536 (1990); see also S. Jorda, U. Rössler, and D. Broido, in Proceedings of the International Meeting on the Optics of Excitons in Confined Systems, 1991, edited by A. D'Andrea, R. Del Sole, R. Girlanda, and A. Quattropani (The Institute of Physics, in press).

[11]R. Kubo, J. Phys. Soc. Jpn. **12**, 570 (1957).

[12]A. Stahl and I. Balslev, *Electrodynamics of the Semiconductor Band Edge* (Springer-Verlag, Berlin, 1987).

[13]L. C. Andreani and A. Pasquarello, Phys. Rev. B **42**, 8928 (1990); L. C. Andreani, Phys. Scr. **T35**, 111 (1991).

[14]L. C. Andreani, F. Bassani, and A. Pasquarello, *Symmetry in Nature,* edited by G. Bernardini (Scuola Normale Superiore, Pisa, 1989), p. 19.

[15]M. Kohl, D. Heitmann, P. Grambow, and K. Ploog, Phys. Rev. B **42**, 2941 (1990).

[16]L. C. Andreani, F. Tassone, and F. Bassani, Solid State Commun. **77**, 641 (1991).

[17]A. A. Maradudin and D. L. Mills, Phys. Rev. B **7**, 2787 (1973).

[18]T. Kloos, Z. Phys. **208**, 77 (1968); see also R. B. Pettit, J. Silcox, and R. Vincent, Phys. Rev. B **11**, 3116 (1975).

[19]D. Fröhlich, P. Köhler, E. Meneses-Pacheco, G. Khitrova, and G. Weimann, in *Proceedings of the International Meeting on the Optics of Excitons in Confined Systems, 1991* (Ref. 10).

[20]M. W. Berz, L. C. Andreani, E. F. Steigmeier, F. K. Reinhart, Solid State Commun. **80**, 553 (1991).

[21]Y. Segawa, J. Cusano, Y. Aoyagi, S. Namba, D. K. Shuh, and R. S. Williams, in *Proceedings of the 19th International Conference on the Physics of Semiconductors, Warsaw, 1988,* edited by W. Zawadzki (IFPAS, Warsaw, 1989), p. 437.

[22]B. Hönerlage, A. Bivas, and Vu Duy Phach, Phys. Rev. Lett. **41**, 49 (1978).